

An objective analysis of the observed spatial structure of the tropical Indian Ocean SST variability

Dietmar Dommenges

Received: 21 October 2009 / Accepted: 4 March 2010 / Published online: 23 March 2010
© Springer-Verlag 2010

Abstract The observed interannual Indian Ocean sea surface temperature (SST) variability from 1950 to 2008 is analyzed in respect to the spatial structure of the variability. The analysis is based on an objective comparison of the leading empirical orthogonal function modes against the stochastic null hypothesis of spatial red noise (isotropic diffusion). Starting from this red noise assumption, the analysis searches for those structures that are most distinct from the red noise hypothesis. This objective approach will put previously well and less known modes of variability into the context of the multivariate SST variability. The Indian Ocean SST variability is marked by relatively weak SST variability, which is strongly dominated by a basin wide monopole pattern that is caused by different processes. The leading modes of variability are the El Niño Southern Oscillation (ENSO) variability and the warming trend, which both project onto the basin wide monopole structure. Other more characteristic spatial patterns of internal variability are much less dominant in the tropical Indian Ocean, which is quite different from all other ocean basin, where characteristic teleconnection patterns exist. The remaining, ENSO independent, detrended variability is dominated by multi-pole patterns from the southern Indian Ocean reaching into the tropical Indian Ocean, which are probably primarily caused by extra-tropical atmospheric forcings. The large scale tropical Indian Ocean internal variability itself has no dominant structure. The currently often used dipole mode index (DMI) does not appear to present a dominant teleconnection pattern of the Indian

Ocean internal SST variability. In the context of the objective analysis presented here, the DMI partly reflects the ENSO variability and is also a representation of the multi-dimensional, chaotic spatial red noise (isotropic diffusion) process. As such the DMI cannot be interpreted as a coherent teleconnection between the two poles.

1 Introduction

The Indian Ocean sea surface temperature (SST) variability has been the focus of many studies over the last decades. A comprehensive recent overview is given in the review article by Schott et al. (2009). It is now believed that the Indian Ocean SST variability is involved in many different aspects of climate variability not only in the Indian Ocean region (e.g. Nicholls 1989; Latif et al. 1999; Bader and Latif 2003; Annamalai et al. 2005), but even on remote regions, such as the northern North Pacific (e.g. Deser et al. 2004) or even very remote as in the North Atlantic-European region (e.g. Bader and Latif 2003). The Indian Ocean SST plays also an active role in the El Niño Southern Oscillation (ENSO) mode (e.g. Wu and Kirtman 2004; Kug and Kang 2006; Dommenges et al. 2006; Jansen et al. 2009).

The SST variability in the Indian Ocean is thought of as being fit into three categories: externally forced, remotely forced or intrinsic to the Indian ocean–atmosphere coupled system. The externally forced SST variability is mainly a basin wide warming trend, mostly caused by the anthropogenic greenhouse gas forcings (e.g. Barnett et al. 2005). The dominant remote forcing comes from the ENSO-mode, which influences the SST variability in the Indian quite significantly (e.g. Bjerknes 1969; Weare 1979; Latif and Barnett 1995).

D. Dommenges (✉)
Leibniz Institute of Marine Sciences, IFM-GEOMAR,
Düsternbrookerweg 20, 24105 Kiel, Germany
e-mail: ddommenget@ifm-geomar.de

Finally, in recent years it has been argued that some significant modes of ocean–atmosphere coupled SST variability exist in the Indian Ocean, independent of the ENSO mode (Saji et al. 1999; Webster et al. 1999). This is namely the Indian Ocean Dipole (IOD) mode, which is defined by the dipole mode index (DMI). The authors mainly argue that this mode of SST variability represents a phenomenon, which is in its main characteristics intrinsic to the Indian Ocean, but involves feedbacks similar, but also partly different, to those causing the ENSO mode in the equatorial tropical Pacific Ocean (Li et al. 2003). These are namely the so-called Bjerknes-feedbacks. The IOD mode is thought of being the dominant mode of SST variability intrinsic to the Indian ocean–atmosphere coupled system.

However, some studies dispute that this DMI does represent a coupled ocean atmosphere mode of SST variability similar to ENSO (e.g. Dommenget and Latif 2002; Dommenget 2007; Jansen et al. 2009). The arguments in Dommenget and Latif (2002) are mainly based on how the empirical orthogonal function (EOF)-modes of the Indian Ocean SST variability can be interpreted. While Saji et al. (1999) and Behera et al. (2003) argue that EOF-1 is the Indian Ocean response to ENSO and EOF-2 the IOD mode, Dommenget and Latif (2003) argue that this interpretation is not correct, but that the EOF-modes tend to be a superposition of many modes or are a representation of a high-dimensional chaotic process (Dommenget 2007). The dispute on how the EOF-mode of the tropical Indian Ocean shall be interpreted is still somewhat unsettled. It therefore seems adequate so take a close look at the modal structure of the SST variability in the tropical Indian Ocean, in order to understand the structure of the leading modes variability.

Despite the large interest in the Indian Ocean SST variability over the recent years, only a few studies have focused on objective analysis of the spatial modes of SST variability and their time scale characteristics (e.g. Weare 1979). An objective analysis of the SST variability is an exploratory analysis without any a priori assumptions of the structures or processes involved in SST variability. It basically starts from the assumption that the data is pure noise and hopes to discover structure in the data distinct from this. This approach is in contrast to most studies, which usually focus on the so called confirmatory analysis, trying to test a physically motivated hypothesis.

The aim of this study is to present an objective analysis of the spatial modes of SST variability and their time scale characteristics. The analysis shall not make any prior assumptions about the nature of the SST modes, but should purely be motivated by the results of the objective analysis of the SST variability as such. After a short description of the data used, the approach of this study is laid out in more

detail in Sect. 3. This is followed by a first analysis of the SST variability and the mean state conditions. The central part of this article is the analysis of the modal structure of the SST variability in Sect. 5, which is divided into several subsections. The study concludes with a summary and discussions section.

2 Data

The analysis presented here is based on observed SST for the period 1870–2008 taken from the HADISST data set (Rayner et al. 2003). However, for the largest part of the analysis only the period 1950–2008 is used, since data prior to this period are less reliable. The 10 m wind climatology is taken from the NCEP reanalysis data from 1950 to 2008 (Kalnay et al. 1996).

3 Approach

The analysis of the modal structure of climate variability is often based on EOF-analysis, which however has some important limitations if it comes to the interpretation of the EOF-modes in terms of the physical processes causing these modes (e.g. Richman 1986; Dommenget and Latif 2002; Monahan et al. 2009). Many different alternative presentations of the leading modes of high dimensional data fields have been proposed and applied to improve the identification of the leading modes of climate variability (e.g. Richman 1986; Jolliffe 2002; Hannachi et al. 2007), where each of these methods have their advantages and disadvantages.

The discussion of the interpretation of the IOD gives a good example on what the problem in the interpretation of statistical modes is (Dommenget and Latif 2002; Dommenget and Latif 2003; Dommenget 2007). In summary the physical interpretation of any single EOF-mode (or any other statistical mode) strongly depends on how the other EOF-modes are interpreted. Understanding a single EOF-mode can only be achieved in the context of all leading EOF-modes. In this context Dommenget (2007) proposed that the EOF-analysis shall be discussed in the context of a multivariate stochastic null hypothesis.

The analysis presented here will be based on EOF-analysis following the recently published strategy of Dommenget (2007). The main assumption (null hypothesis) of Dommenget (2007) is that the EOF-modes are considered as a representation of a continuous spectrum of spatial patterns resulting from a stochastic process. In this continuous spectrum of spatial patterns all possible spatial structures exist, but some are more dominant than others. This is analogue to the red noise spectrum of time series, in

which low frequency oscillations are more dominant than high frequency oscillations, but no preferred dominant period exist. The spatial climate field analogue to the Hasselmann (1976) null hypothesis of red noise for climate time series is the isotropic diffusion process, which has a red noise spatial spectrum, but no preferred spatial teleconnection pattern. As in the Hasselmann (1976) null hypothesis the driving forcing is the weather fluctuations. The spatial reddening of weather forcing in the isotropic diffusion null hypothesis may either be done by atmospheric or oceanic effective diffusivity, which is unlike the Hasselmann (1976) model, where reddening comes only from the slow system.

In this isotropic diffusion process null hypothesis the EOF-modes are not interpreted as teleconnections, but as reflections of different spatial scales. A basin wide monopole EOF-1, for instance, would represent the largest possible scale in the domain and has therefore the largest variance. A basin wide dipole EOF-2 mode is the second largest scale orthogonal to the EOF-1 and would, in the context of the stochastic isotropic diffusion model, be interpreted as variability of half-basin width scale, but not as a teleconnection with coherent variability of opposite sign in the two peaks of the EOF-pattern. Thus in the stochastic isotropic diffusion model no teleconnections exist, other than the most trivial, that nearby regions are more similar in their variability than more remote regions. Deviations from this stochastic isotropic diffusion null hypothesis are then considered to be the interesting structure of the data field, which in some cases may be interpreted as the leading teleconnections.

The method of Dommenget (2007) is based on normal EOF-analysis, which is then compared against a fitted isotropic diffusion process. The deviations of the eigenvalue (EV) spectrum of the data from the fitted isotropic diffusion process points to the EOF-modes that explain more variance than expected under the isotropic diffusion null hypothesis. By rotating the leading EOF-modes, the modes that are most distinguished (referred to as DEOFs) from the isotropic diffusion null hypothesis can be found. In analogue to the principle component (PC) time series of EOFs, the time series of the DEOFs are referred to as the distinguished principle components (DPCs). More details about the methods, examples and how it is applied to data fields are given in Dommenget (2007).

In summary, the following analysis starts from the null hypothesis that no teleconnections in the tropical Indian Ocean exist and that the SST variability is just a spatial red noise spectrum (a stochastic isotropic diffusion process). The EOF-modes are assumed to be representation of red noise and deviations from this null hypothesis will point to the leading teleconnections, or more generally, to more interesting processes.

4 Indian Ocean SST variability

Before we start the more complex analysis of the modal structure of SST variability in the Indian Ocean it is instructive to have a first look at some snap shots of monthly mean SST anomalies in the wider area of the tropical Indian Ocean to get some non-parametric view of the spatial structure of SST anomalies, see Fig. 1. The snap shots are picked mostly randomly, but strong El Nino or La Nina month are avoided to better highlight Indian Ocean SST variability (any other random set should roughly give the same characteristics, as discussed below). From these random snap shots we can recognize some (known) structures of the tropical Indian Ocean SST variability, which will be quantified in the subsequent analyses following below:

- First the influence of El Nino is present. Strong SST anomalies in the equatorial Pacific lead in general to basin wide SST anomalies of the same sign in the tropical Indian Ocean (see, for instance, Fig. 1 3/1971 or 5/1983).
- We can also recognize some stronger SST anomaly patterns in the southern extra-tropical Indian Ocean (see, for instance, Fig. 1 2/1968 or 3/1974).
- The tropical Indian Ocean SST anomalies are relatively weak if compared to those in neighboring domains (e.g. tropical Pacific or southern extra tropical Indian Ocean). SST anomalies larger than 0.5 K are rare.
- No obvious pattern of SST variability is visible in the tropical Indian Ocean, accept for a basin wide monopole.

The strength of the SST variability can be estimated by the standard deviation of monthly mean linear detrended SST, see Fig. 2. The tropical regions are marked by two equatorial regions of enhanced SST variability in the central to eastern equatorial Pacific and Atlantic. Both are related to the El Nino-like ocean-atmosphere interaction. Further we can see enhanced variability in the coastal regions on the eastern sides of the Pacific and Atlantic, which is related to small scale coastal upwelling variability. Some coastal variability is also visible in the Indian Ocean in the east near Java and Sumatra and in the west along the African and Arabian coasts. Outside these regions is the tropical SST variability significantly weaker, with the variability generally increasing towards high latitudes. The tropical Indian Ocean (off the coasts) has more or less homogenously weak SST variability, with no specific structure. It marks the Ocean domain with the weakest SST variability compared to all other global ocean domains. This, however, does not necessarily mean that the SST variability is less important, since regions with warmer mean SST, as in tropical Indian Ocean, will in general

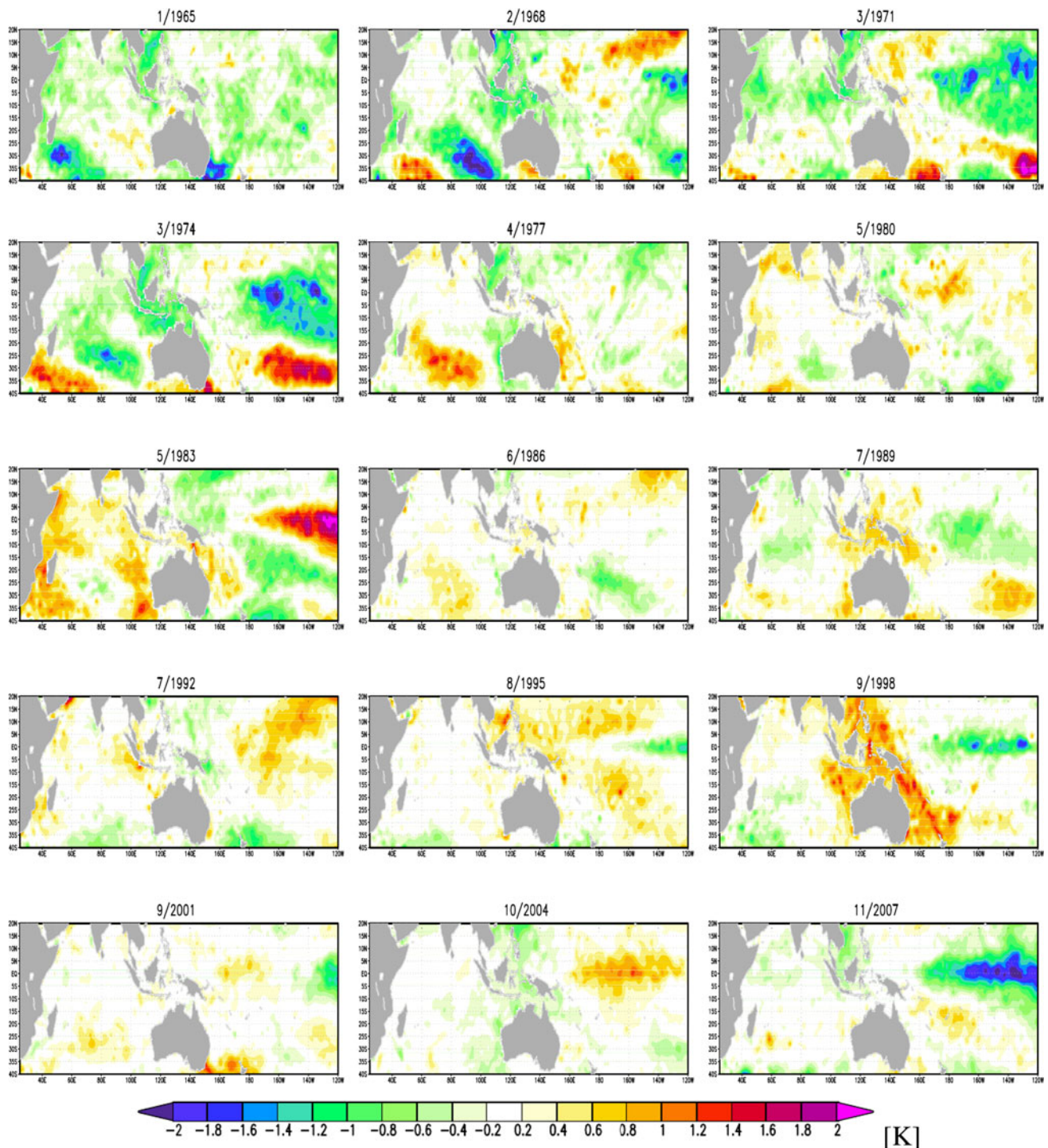


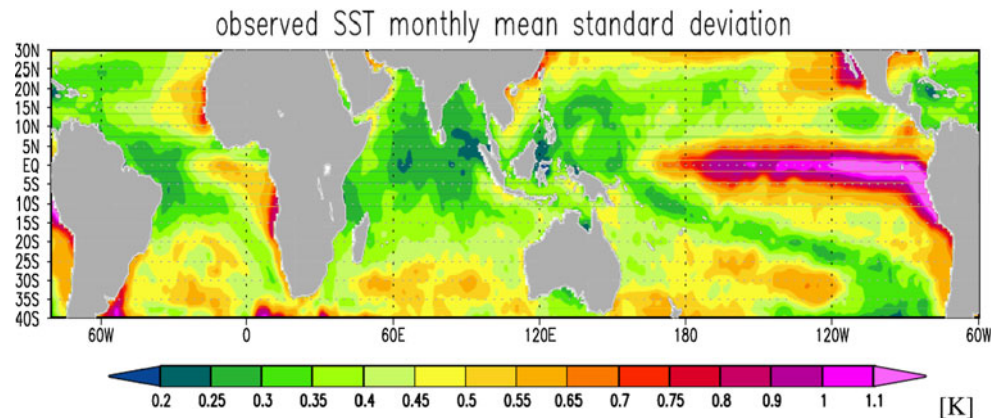
Fig. 1 Random snap shots of linear detrended monthly mean SST anomalies, avoiding months with strong El Nino/La Nina events, to better highlight Indian Ocean SST anomalies

lead to a stronger latent heat response for a given SST anomaly amplitude, than regions with colder mean SST.

Figure 3a,b shows the mean temperature field of the three tropical oceans for the warmest (spring) and coldest season (summer) of the Indian Ocean SST. We can note that both the Pacific and the Atlantic Ocean have a

pronounced east to west temperature gradient, caused by the eastern boundary and equatorial up-welling cold tongues. In contrast, the Indian Ocean mean SST is much more uniformly warm with the warmest temperature on the equator and at the eastern boundaries, but with some colder upwelling regions at the western boundary (most

Fig. 2 Standard deviation of linear detrended monthly mean SST anomalies for the time period 1950–2008



pronounced in the boreal summer season). Along with the cold tongues in the Pacific and the Atlantic Ocean goes enhanced SST variability as measured by the standard deviation of the linear detrended SST anomalies (see Fig. 2). This most characteristic feature is clearly missing in the Indian Ocean.

5 The modal structure of Indian Ocean SST variability

In order to analyze the spatial and temporal structure of the Indian Ocean SST variability by means of EOF-analysis we have to choose the domain boundaries. To the west and north the boundaries are well defined by continents. To the east the main islands and Australia may define a natural boundary relatively well, but there may be some discussion of whether or not the seas east to Java and Sumatra shall be included or not. For the analysis discussed in the following all SST west of 120°E are included, but all EOF analysis results are double checked with SST east of the Malay Peninsula, Java and Sumatra excluded. None of the results discussed in the following analysis is sensitive to the exclusion of the SST in this area.

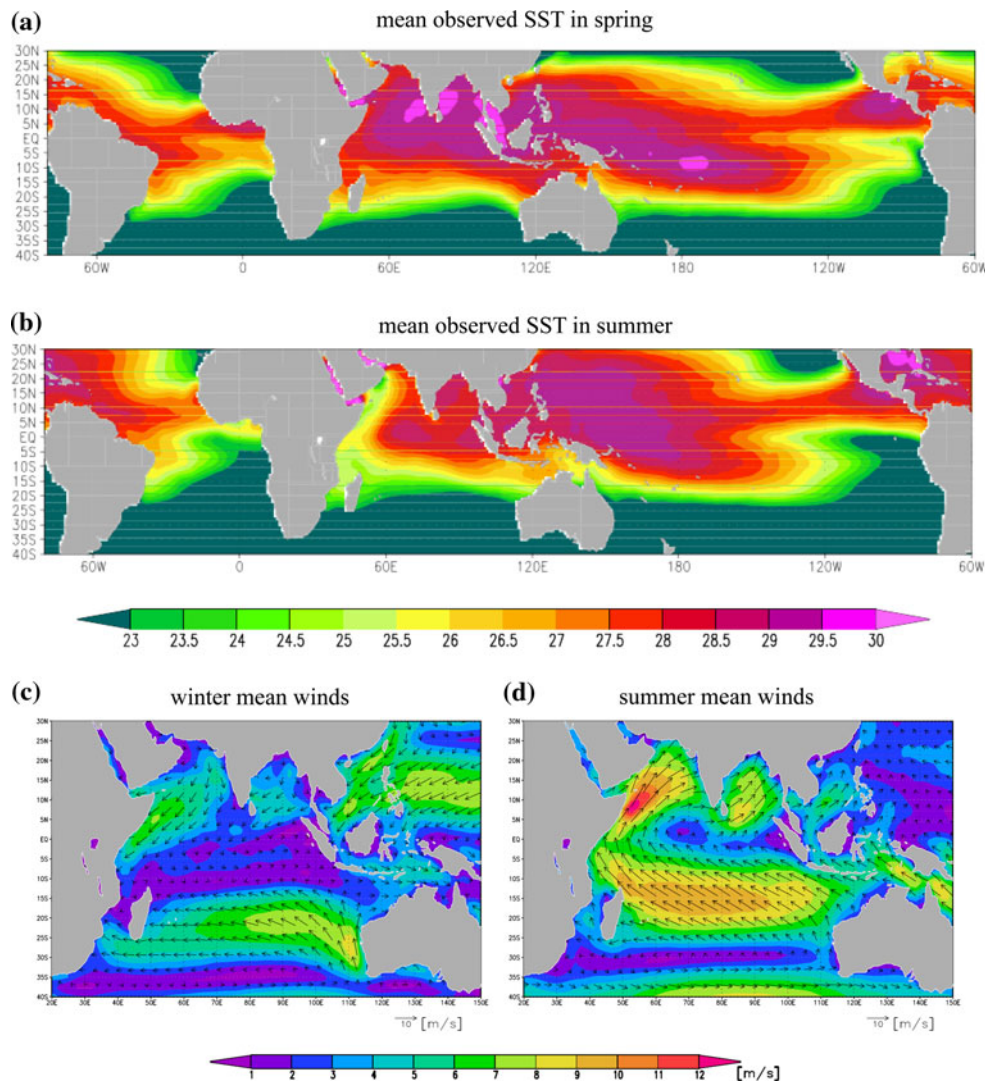
To the south, however, no natural boundary exists and any choice for a domain boundary may be somewhat arbitrary. To motivate a starting point for the EOF-analysis, we can have a look at the mean SST and wind fields, which give some idea of the main atmospheric forcing conditions (see Fig. 3). The warm (above 25°C) SST ends at about 15°S–20°S, depending on the season. Further, the center of the southern trade winds may provide a natural separation between tropical SST variability to the north, from extra-tropical SST variability to the south. This boundary moves during the seasonal cycle somewhere between 20°S and 15°S. In the literature the boundary for EOF-analysis has often been set at about 20°S. The relevance of the southern boundary on the definition of the SST modes will be discussed during the now following EOF-analyses.

We therefore start the analysis with the EOF-modes of the unfiltered SST anomalies from 1950 to 2008 as in Dommenget (2007) with the southern boundary at 20°S, see Fig. 4. Note that the data is not detrended a priori, although a linear trend in tropical Indian Ocean is a well known feature. The approach here is to objectively analyze the data with as little as possible a priori assumptions. The analysis shall by itself detect the linear trend as a significant feature of the SST data.

The EOF-modes of the unfiltered SST anomalies are characterized by a clearly dominating monopole structure in EOF-1, followed by a much less dominant mode of a zonal dipole, which is stronger in the off-equatorial regions and most strongest on the southern hemisphere. The EV spectrum is characterized by the dominating first eigenvalue, followed by a series of higher order eigenvalues, which appear to be decreasing more continuously. The dominance of the first eigenvalue leads to the relative small number of effective spatial degrees of freedom of $n_{\text{spatial}} = 4.1$, as estimated by the criteria of Bretherton et al. (1999).

Following the approach of Dommenget (2007) the eigenvalue spectrum can be compared against an isotropic diffusion process to evaluate the potential physical processes causing the EOF-modes (see previous section for details). Therefore the EOF-modes of the isotropic diffusion process fitted to the SST data are projected on those of the SST data, resulting into an explained variance value for each of the SST data eigenvalues (see red line in Fig. 4d). The eigenvalue spectrum of the leading modes is in relative good agreement with the null hypothesis of an isotropic diffusion process (a spatial AR(1)-process) as noted in previous studies (Dommenget 2007; Hannachi and Dommenget 2009). The spatial red noise hypothesis (red line in Fig. 4d) is roughly a fluctuation around the observed eigenvalues (black line in Fig. 4d). This first of all means, that the structure of the Indian Ocean SST variability is similar to an isotropic diffusion process with basin wide variability dominating.

Fig. 3 Mean SST in spring (AMJ) **(a)** and summer (JAS) **(b)** over the period 1950–2008. **c** Mean 10 m winds in the winter (DJF) season. **d** Mean 10 m winds in the summer (JJA) season. Winds are taken from the NCEP reanalysis



In the context of the EOF-2 mode or the IOD or DMI, the interpretation would be that this index would not represent a preferred structure of the Indian Ocean SST variability, which is not already included in an isotropic diffusion process. It thus is a reflection of the continuous spectrum of spatial patterns of SST variability, which in an isotropic diffusion process would prefer larger scale structures such as a domain wide monopole or dipoles. The DMI (roughly EOF-2), has actually slightly less variance than would be expected from the continuous spectrum of patterns of a purely isotropic diffusion process.

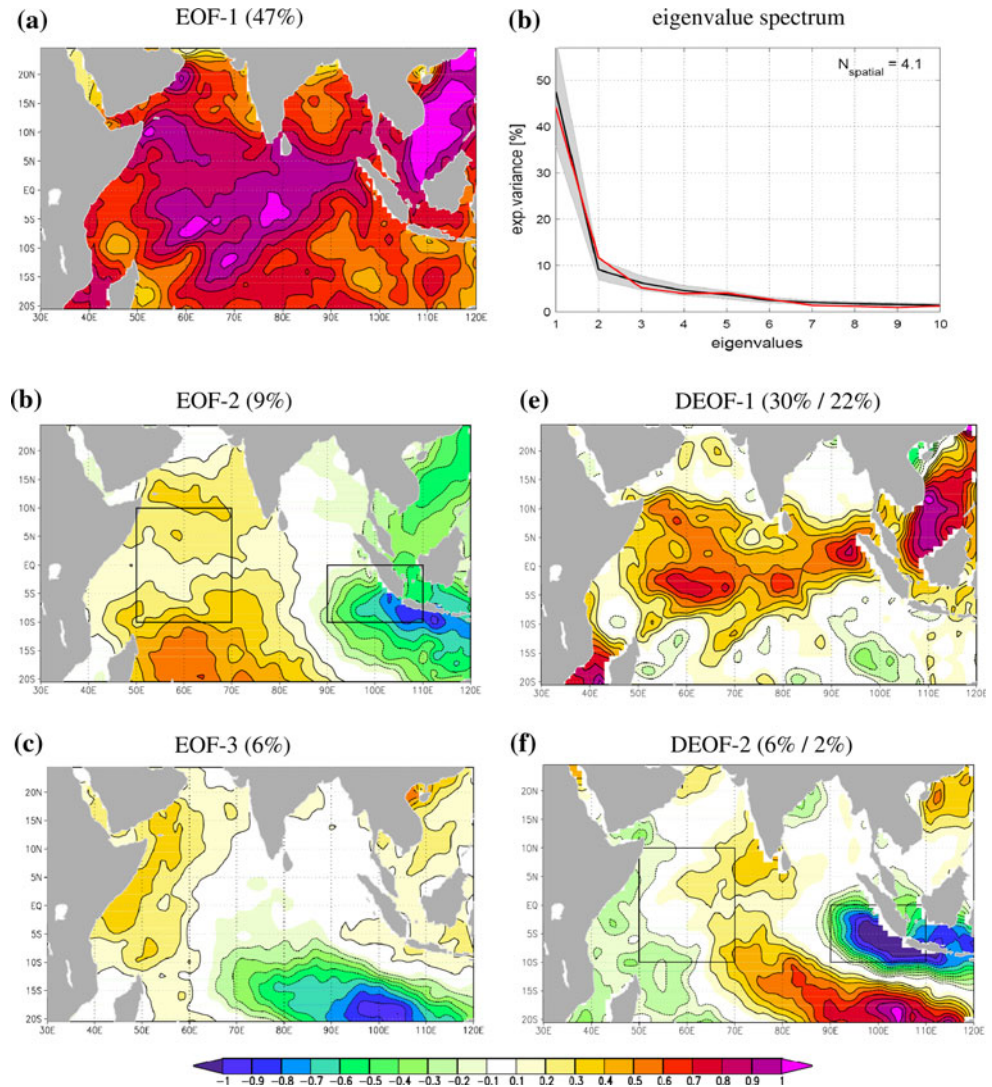
To understand this result better it is instructive to look at the results of EOF-analyses in comparison with an isotropic diffusion process for other ocean domains, see Fig. 5. Note, that here the period 1870–2008 based on annual mean SST variability is used to better represent the decadal variability in the North Pacific and Atlantic, but the results are essentially the same, in the context of this analysis, with the

EOF-analysis restricted to the period 1950–2008 based on monthly mean SST anomalies.

In all other ocean basin domains we find stronger deviations of the eigenvalues from the fitted isotropic diffusion process, than in the tropical Indian Ocean domain. This means that in all ocean domains more significant spatial structures of variability exist, than in the tropical Indian Ocean (if we do not consider a basin wide monopole as significant spatial structure). Further we find that in all ocean basins the most significant structures found (the DEOF-1) are those discussed in the literatures as being the leading modes of variability. All rotated DEOFs discussed in this study are based on the first 20 EOF modes and all features discussed in the following are robust against the alteration of the number of EOFs used for the rotation.

In the tropical Pacific the EOF-analysis finds a central Pacific El Nino-like pattern to be the most significant structure of variability (see also Dommenget 2007), which

Fig. 4 EOF-analysis of the unfiltered SST anomalies from 1950 to 2008. **a–c** The leading 3 EOF-patterns with the explained variance of each mode in the heading of *each panel*. **d** EV-spectrum (*black solid line*) together with the projected isotropic diffusion null hypothesis (*red line*). The *shaded area* marks the uncertainty interval of the eigenvalues after North et al. (1982). **e–f** The leading DEOF-patterns resulting from the rotation of the leading EOFs in order to maximize the difference between the explained variance of the patterns (first number in the heading of the panels **e** and **f**) and that expected for the isotropic diffusion null hypothesis (second number in the heading of the panels **e** and **f**). The DMI regions are plotted for comparison in panels **b** and **f**. Contours in all panels are in arbitrary units



is clearly in agreement with the general understanding of tropical Pacific SST variability. The analysis of the tropical Atlantic EOF-modes also finds the equatorial Atlantic El Nino type of pattern to be the most dominant structure deviating from isotropic diffusion process, which is in agreement with other analysis (e.g. Zebiak 1993). Note, that this pattern also projects somewhat on the tropical Atlantic interhemispheric dipole pattern, suggesting that some more complex teleconnections beyond the Atlantic El Nino type of pattern may exist here.

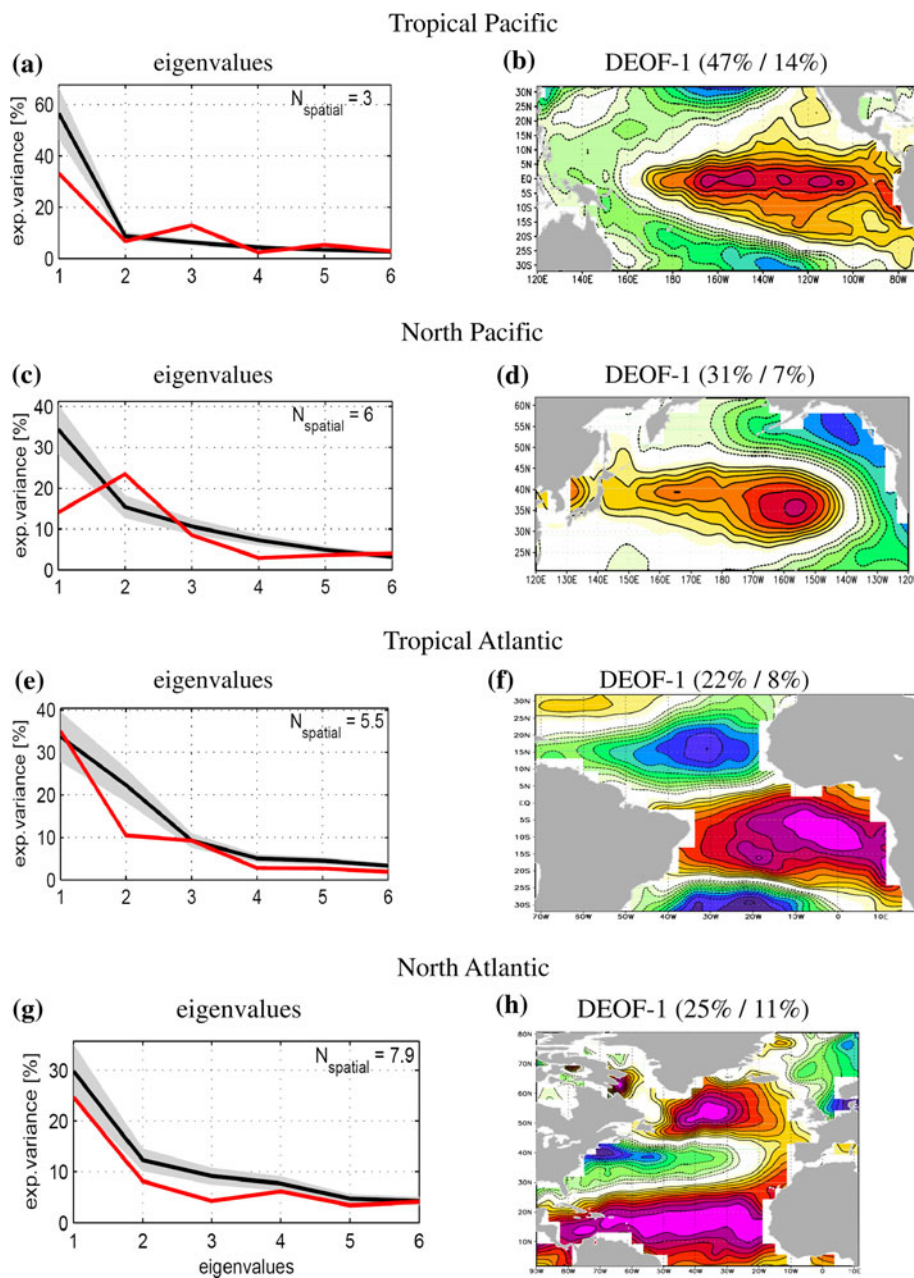
In the North Pacific a Pacific Decadal Oscillation (PDO) type of pattern emerges as the most important pattern, which is also in agreement with the literature (e.g. Mantua et al. 1997) and in the North Atlantic the leading modes of variability is the ‘horseshoe’ type of pattern, which is related to the dominant forcing by the North Atlantic Oscillation (NAO) and is in general assumed to be the dominant pattern of interannual to decadal variability (e.g. Marshall et al. 2001). The southern Ocean (not shown) also

shows strong deviations from the fitted isotropic diffusion process, with the leading pattern being related to the El Nino variability, but due to the sparse data in this region little can be said about the significance of this result. In summary, we find that all ocean basins show significantly stronger deviations from the isotropic diffusion process null hypothesis in the leading EOF-modes, than those found for the tropical Indian Ocean.

Although the tropical Indian Ocean SST variability agrees much better with the isotropic diffusion process null hypothesis than any other ocean basin, we cannot conclude that the SST variability in this domain is caused by isotropic diffusion (see also Hannachi and Dommenget 2009). It just means that a dominant mode of variability in this domain is not as obvious and strong as in other ocean basins.

We therefore continue the analysis with looking at those structures that deviate the most from the isotropic diffusion null hypothesis. The spatial pattern that deviates the most

Fig. 5 EV-spectrum (*left column*) and DEOF-1 pattern (*right column*) for different ocean basins based on annual mean exponentially detrended SST for the period 1870–2008. As in Fig. 4d, the EV-spectrum (*black solid line*) is shown together with the projected isotropic diffusion null hypothesis (*red line*). The shaded areas in the EV-spectrum mark the uncertainty interval of the eigenvalues after North et al. (1982). As in Fig. 4e–f the first number in the heading of the *right-hand side* panels is the explained variance of the DEOF-1 and the second that expected for the isotropic diffusion null hypothesis



from the spatial AR(1)-process (DEOF-1 in Fig. 4e) is a central monopole structure similar to EOF-1. Note that in a domain with very few degrees of freedom, as in the tropical Indian Ocean SST, a monopole teleconnection pattern will be very close to the fitted isotropic diffusion process, since it can simply not be distinguished from isotropic diffusion with very large (basin wide) decorrelation length. The fact that the DEOF-1 still points to the monopole must be considered as a good indication that this monopole pattern represents indeed a deviation from the null hypothesis.

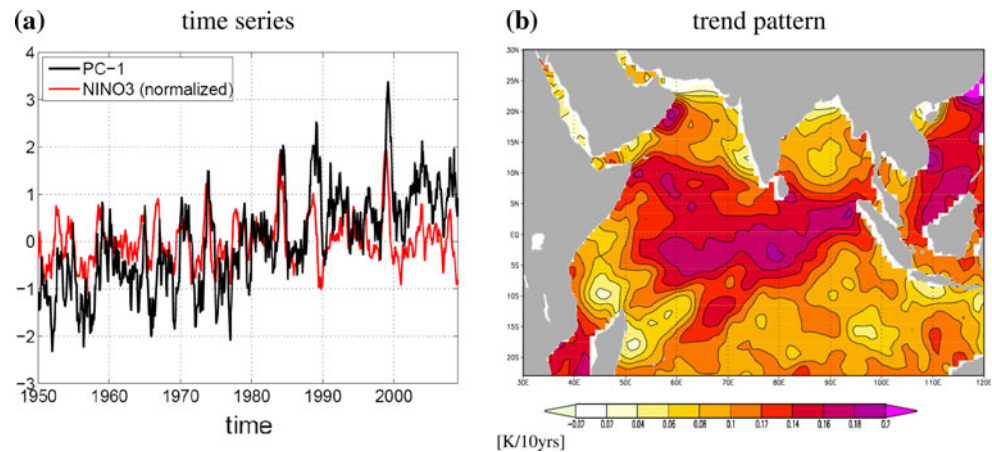
The DEOF-2 marks a south-west to north-east multipole in the southern hemisphere, but deviations from the spatial AR(1)-process are small. Two influences to the

tropical Indian Ocean have been discussed in the literature, that are of a monopole type of structure: The response to El Niño and the warming trend of the SST over the past decades. These two influences are discussed in more detail in the following analysis.

5.1 Trend

Figure 6a shows the time series of the PC-1 of the EOF-analysis shown in Fig. 4. The time series shows a clear linear warming trend, supporting the idea that the monopole type of structure of EOF-1 is partly caused by the linear warming trend in tropical Indian Ocean. The linear

Fig. 6 **a** Time series of the PC-1 of the EOF-1 as shown in Fig. 4a (black line) and the normalized NINO3 SST index (red line). **b** Linear trend pattern estimated from 1950 to 2008



warming trend in the tropical Indian Ocean can be estimated by a linear regression over the period 1950–2008. The trend pattern shows a basin wide warming with largest amplitudes over the central equatorial Indian Ocean, see Fig. 6b. The pattern is very similar to EOF-1 or DEOF-1, as already noted in Hannachi and Dommenges (2009). The linear warming trend explains about 24% of the total variance of SST variability in the tropical Indian Ocean, most strongly over the central equatorial Indian Ocean. The time evolution of the trend pattern (not shown) is highly correlated (>0.98) to that of PC-1 and DPC-1 (not shown). Thus, the first mode of variability that is found is the warming trend.

We can now repeat the EOF-analysis on the linear detrended SST anomalies from 1950 to 2008, see Fig. 7. While the leading EOF-patterns have not changed that much, the eigenvalue spectrum is now more continuous, with the EV-1 explaining much less variance than before and the higher order modes explain relatively more variance than before (compare with Fig. 4d). Subsequently the effective number degrees of freedom have increased by almost a factor of two ($n_{\text{spatial}} = 7.6$). The EV-spectrum is still in relative good agreement with the spatial AR(1)-process, but most leading eigenvalues tend to have slightly more variance, than expect for the spatial red noise hypothesis. This indicates some deviation from the fitted red noise null hypothesis. The DEOFs again point to approximately the same two patterns. The two patterns show about equally strong deviations from the spatial AR(1)-process, but the DEOF-1 explains overall much more variance. The results of this EOF-analysis therefore suggest that a second important mode of variability that projects onto EOF-1 or DEOF-1.

5.2 ENSO influence

The time series of PC-1 or DPC-1 of the unfiltered or detrended SST does show some significant interannual

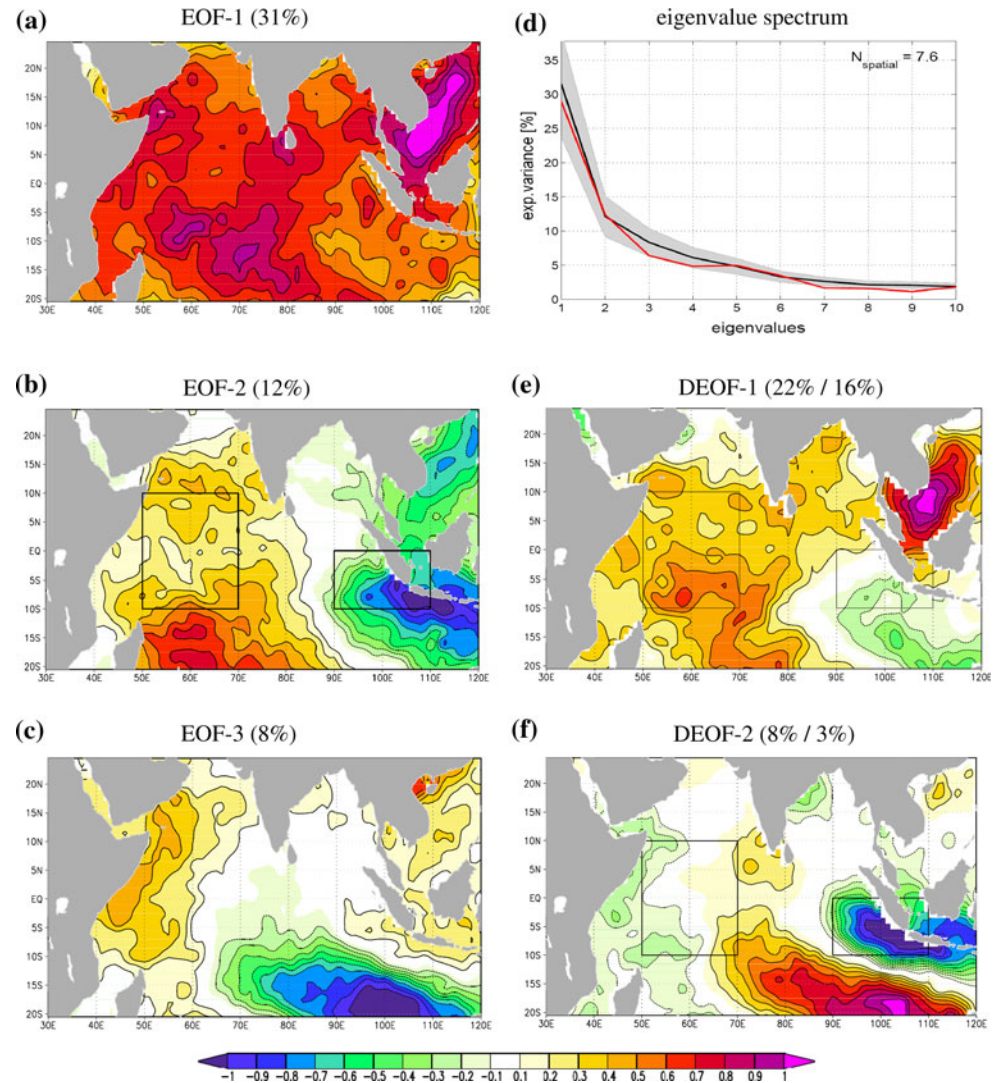
variability, which is related (correlation 0.6) to the NINO3 time series (see Fig. 6a). The ENSO impact on the Indian Ocean can first be roughly estimated by the correlation with the NINO3 SST time series, see Fig. 8a,b. Since the ENSO teleconnections are changing over the seasons, the correlation is shown for winter and fall season to contrast the most distinct seasons. The correlation pattern in the Indian Ocean in the winter time is very similar to the EOF-1 or DEOF-1. In the fall season it is more of a dipole pattern with warming in most of the tropical Indian Ocean and cooling in the southeast Indian Ocean. This suggests that the response to ENSO is not just a fixed pattern, but evolves seasonally and also during the ENSO cycle, as has been noted in previous studies.

In order to quantify the ENSO variability in the Indian Ocean and in order to define the SST variability in the tropical Indian Ocean that is, to a first order approximation, independent of ENSO, SST_{deENSOed} , we can estimate the ENSO variability in the Indian Ocean SST by a simple linear regression model with seasonally varying regression parameters, as done in Kug et al. (2004). The detrended SST at any time, t , can be assumed to be a function of the NINO3 SST at t or at some time lag of maximal 12 month before t :

$$SST_{\text{deENSOed}}(t) = SST(t) - \sum_{\tau=0}^{12} r(\tau, m) \cdot SST_{\text{NINO3}}(t - \tau)$$

The ENSO independent part of the detrended SST, SST_{deENSOed} , is the residual of the multivariate regression with the SST in the NINO3 region, SST_{NINO3} , with the regression parameter, r , as a function of lag time, τ , and calendar month, m . Note that this linear regression model does not tell about causality. Although the main cause of the ENSO variability is in the tropical Pacific, some minor, but important, feedback from the Indian Ocean onto ENSO seem to exist (e.g. Wu and Kirtman 2004; Kug and Kang 2006; Dommenges et al. 2006; Jansen et al. 2009). Thus the

Fig. 7 As in Fig. 4, but for the EOF-analysis of the linear detrended SST anomalies from 1950 to 2008



Indian Ocean SST variability associated with ENSO is not just a response, but would be better described as ENSO coupled variability. Further, it has to be noted that this linear model neglects the non-linear aspects of ENSO, which in some cases may be relevant.

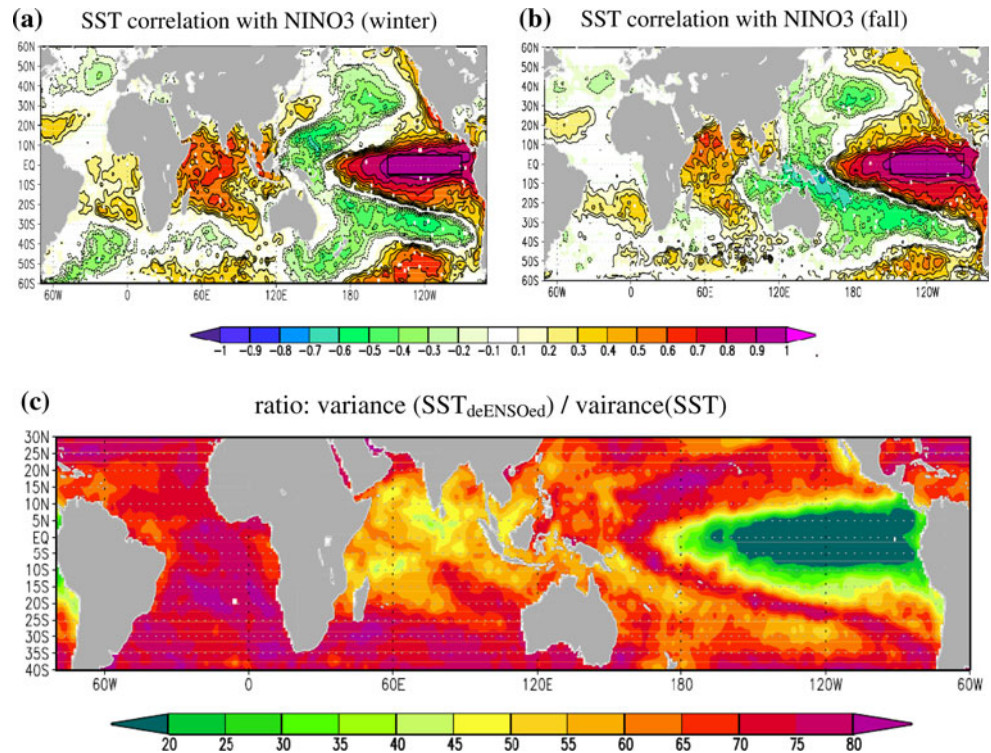
Figure 8c shows the variance ratio of the ENSO-residual relative to the total linear detrended SST variance. The influence of ENSO onto the tropical Indian Ocean SST variability is quite substantial. It shows the strongest response to NINO3 SST outside the tropical Pacific. About 40–60% of the detrended SST variance in the Indian Ocean may be attributed to the ENSO-mode. Although many previous analyses focused on the ENSO influence on the Indian Ocean SST (e.g. Venzke et al. 2000; Shinoda et al. 2004; Behera et al. 2006), only few of them quantify directly or indirectly the amount of SST variability caused by ENSO (e.g. Baquero-Bernal et al. 2002; Kug et al. 2004; Penland and Matrosova 2006; Compo and Sardeshmukh 2010). The results of these studies, using very different

approaches to estimate the ENSO impact onto Indian Ocean, seem to generally agree well with the result of this study, although Compo and Sardeshmukh (2010) argue that a multi-dimensional ENSO could explain much more of the tropical SST variance. The ENSO influence is therefore the strongest mode of variability in the tropical Indian Ocean, followed by the warming trend.

5.3 Tropical Indian Ocean internal variability

We can now discuss the SST variability independent of the warming trend (detrended) and the ENSO-variability (deENSOed), which may be considered as the tropical Indian Ocean internal variability. The leading EOF-patterns (Fig. 9a–c) are still somewhat similar to the ones of the unfiltered data (Fig. 4), but some significant changes are found. First the EOF-mode, although still a monopole, is now clearly focused within a region in the southern hemisphere. Further the EV-spectrum is now even more

Fig. 8 Correlation of global SST with the NINO3 index for winter (a) and fall (b) month. Panel c shows the ratio in variance for the linear detrended SST variability with the ENSO variability removed ($SST_{deENSOed}$) and the linear detrended SST for the period 1950 to 2008



continuous, than in the detrended case (Fig. 7), with the EOF-1 explaining even less variance than before and the higher order EOFs explaining more variance. Subsequently no real dominant mode of variability exists in this SST variability. Again the effective number degree of freedom has increased by almost a factor of two ($n_{spatial} = 13.2$). We can now also find some more significant deviations of the EV-spectrum from the spatial AR(1)-process. First it can be noted that almost all of the 10 leading EOF-modes explain more variance than expected under the null hypothesis, indicating that now the SST variability has distinct structures deviating from a pure isotropic diffusion process. The DEOF-1 is a significant south to north dipole with the northern pole centered on Indonesia. A third pole in DEOF-1 seems to exist further to the south of the EOF-domain boundary. DEOF-2 also marks a south to north dipole, with the main poles centered at the southern boundary of the EOF-domain.

The time series and the associated spectra of the most pronounced patterns of tropical Indian Ocean internal SST variability are shown in Fig. 10. The variability is dominated by the annual to interannual time scales. It is interesting to note that the anomaly time series seem to have somewhat enhanced variance at the annual time scale, similar to the annual peak found in Möller et al. (2008). In the study of Möller et al. (2008) this peak was mostly related to the midlatitudes process of winter time reemergence of SST variability. It is unclear from the data

analysis presented here, whether this type of mechanism exists in the Indian Ocean as well.

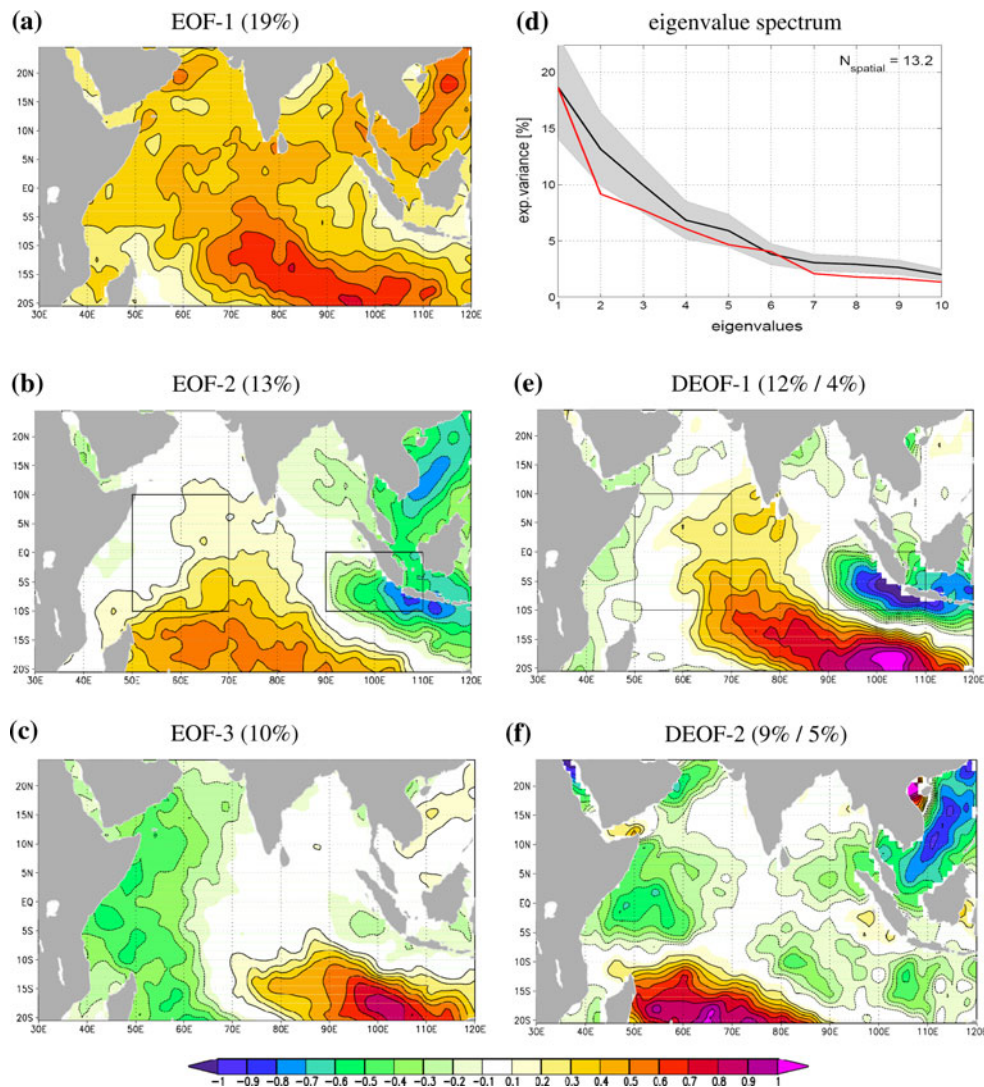
5.4 Southern Indian Ocean

In the above analysis we have found that the leading modes of the internal Indian Ocean SST variability are all near the southern boundary of the analysis domain. This may suggest that these modes have a stronger link to SST variability south of the boundary. Figure 11 shows the correlation of PC-1, DPC-1 and DPC-2 with near global $SST_{deENSOed}$. Both the DPC-1 and DPC-2 have a strong connection to the southern Indian Ocean and cannot be regarded as tropical Indian Ocean SST modes. To further study these modes it is instructive to repeat the EOF-analysis of detrended and deENSOed SST for a domain reaching further south, see Fig. 12. The two leading DEOF modes are essentially the same as for the tropical domain, suggesting that these modes are primarily modes of the southern extra-tropical regions. Note also, that the strongest modes of variability are south of 10°S, which is somewhat expected since the variability increases to the south, as already shown in Fig. 2.

5.5 Seasonal aspects

Many studies of the Indian Ocean SSTs suggest seasonal differences in the SST variability in the different seasons

Fig. 9 As in Fig. 4, but for the linear detrended SST with the ENSO variability removed ($SST_{deENSOed}$)



(e.g. the IOD mode or the ENSO response). We can therefore repeat the EOF-analysis as shown in Figs. 7 and 9, but for all four seasons individually. The seasonality can be summarized by projecting the EOF-modes of the individual seasons onto the all-seasons EOF-modes. So instead of projecting the modes of the fitted null hypothesis onto the data EOF-modes, we now project the modes of the seasonal data onto those of the all-seasons data, testing the null hypothesis that both sets of EOF-modes are essentially the same. This results into estimates of the all-seasons EV-spectrum for each individual season, on the basis of the eigenmodes of the all-seasons EOF-analysis, see Fig. 13.

If we first study the EV-spectrum of the detrended SST (including the ENSO variability) we can find some pronounced seasonality. In the winter and spring seasons the leading EOF-1 (monopole) is more pronounced (explaining more variance in these seasons) and the higher order EOF-modes are less important. The opposite holds for the summer and fall season, here the dipole pattern is more

pronounced, as it has been recognized in other studies as well.

If the analysis is repeated on the deENSOed SST variability we find much smaller differences for the individual seasons. Here the leading SST modes are roughly the same over all seasons. Thus the seasonality is mainly caused by the ENSO-variability, which is more monopole-like in winter and spring, and more like the west-east dipole-like (DMI-like) in summer and fall. That is not to say, that there are no seasonal differences in the deENSOed SST variability. The DEOF-1 mode of the all-seasons the deENSOed SST variability (Fig. 9e), for instance is more pronounced in the JJA and SON seasons.

6 Summary and discussions

In this study the modal structure of the observed interannual Indian Ocean SST variability was analyzed. In contrast to

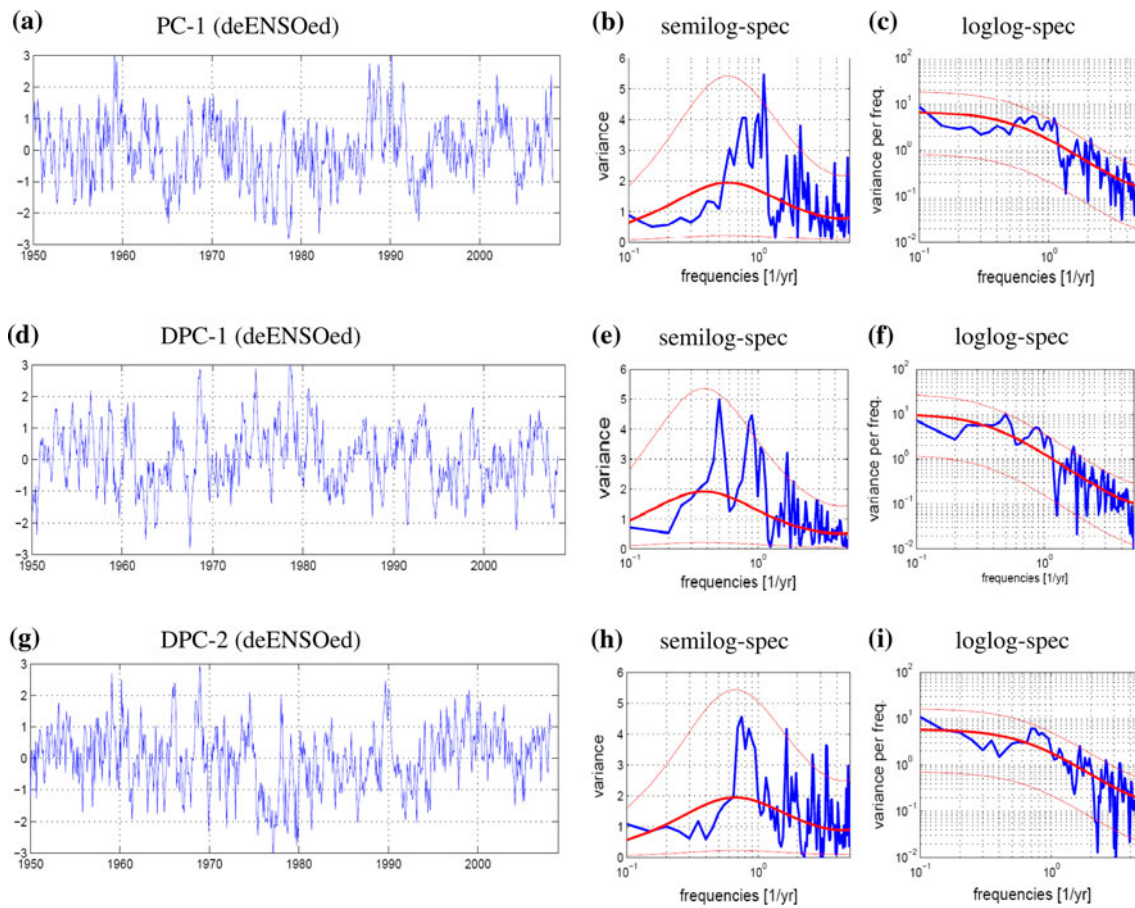


Fig. 10 Time series and the associated spectrum of the PC-1 (a–c), DPC-1(d–f), DPC-2(g–i) of the EOF-analysis presented in Fig. 9. The spectra are presented in a semi-log and log–log presentation. The

thick solid red lines in the spectra are the spectra of the AR(1)-processes fitted to the time series. The *thinner red lines* mark the 95% confidence interval

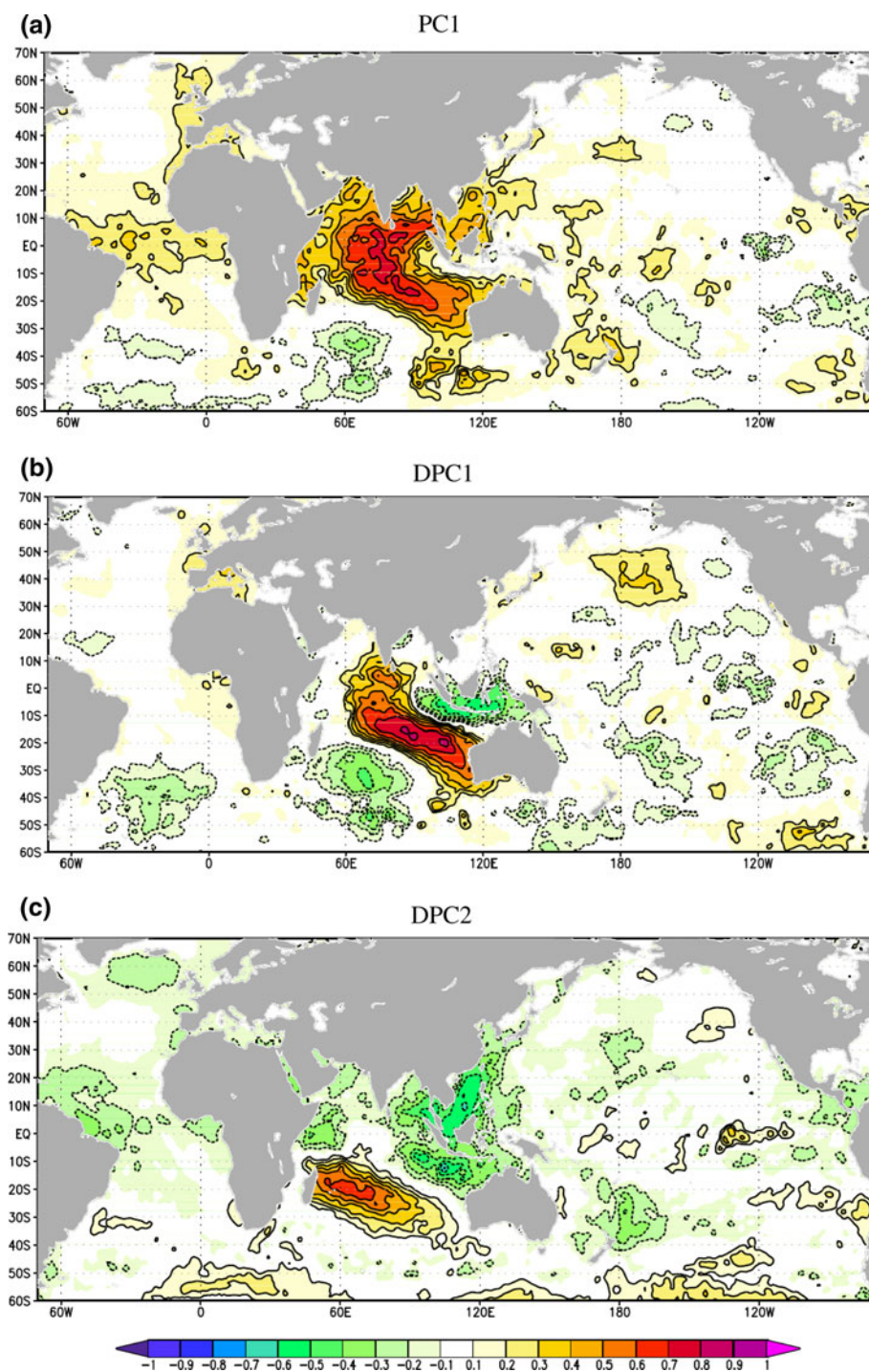
previous studies, that focused on the analysis of a particular phenomenon in the Indian Ocean SST variability (such as the ENSO variability or the IOD mode), the analysis presented here started from the null hypothesis, that the SST variability has no preferred modes of variability other than those expected from an isotropic diffusion process, following the approach of Dommenget (2007). In this more objective approach the multivariate SST variability has been discussed as a whole and the important teleconnection patterns or climate modes have been resulted from the discussion of the complete SST variability.

The basis for this analysis have been the leading EOF-modes of interannual SST variability, which were compared against those of a fitted isotropic diffusion process, representing the spatial analogue to an AR(1)-process (red noise). By examining the multi-dimensional structure of the leading modes, those modes deviating the most from the null hypothesis can be found. These patterns have been taken as the starting points for defining the most dominant modes of variability in the Indian Ocean. It may be noted here that intra-seasonal and smaller scale SST variability may be somewhat neglected by this approach.

The results can be summarized as followed:

- The tropical Indian Ocean SST variability is relatively weak and has only weak spatial structure (domain wide monopoles not considered), in comparison to other ocean basins. It needs to be noted, though, that the weak SST anomaly amplitudes does not necessarily mean that tropical Indian Ocean SST anomalies are not important for global climate variability. It has to be considered that the much warmer Indian Ocean mean state would favor stronger atmospheric responses, due to non-linearities in the latent heat release, if compared to other ocean basins. However, it is remarkable that the tropical Indian Ocean regions is the one with the least amount of variability, which may open up the question, whether the lack of variability in the tropical Indian Ocean may be more interesting, than the present of some small anomalies.
- The leading mode of SST variability in the tropical Indian Ocean is the ENSO variability, which is in general agreement with previous findings (e.g. Latif and Barnett 1995; Schott et al. 2009 and references

Fig. 11 Correlation of the PC-1 (a), DPC-1 (b) and DPC-2(c) time series of the EOF-modes presented in Fig. 9 with global linear detrended ENSO removed SST variability ($SST_{deNSOed}$)

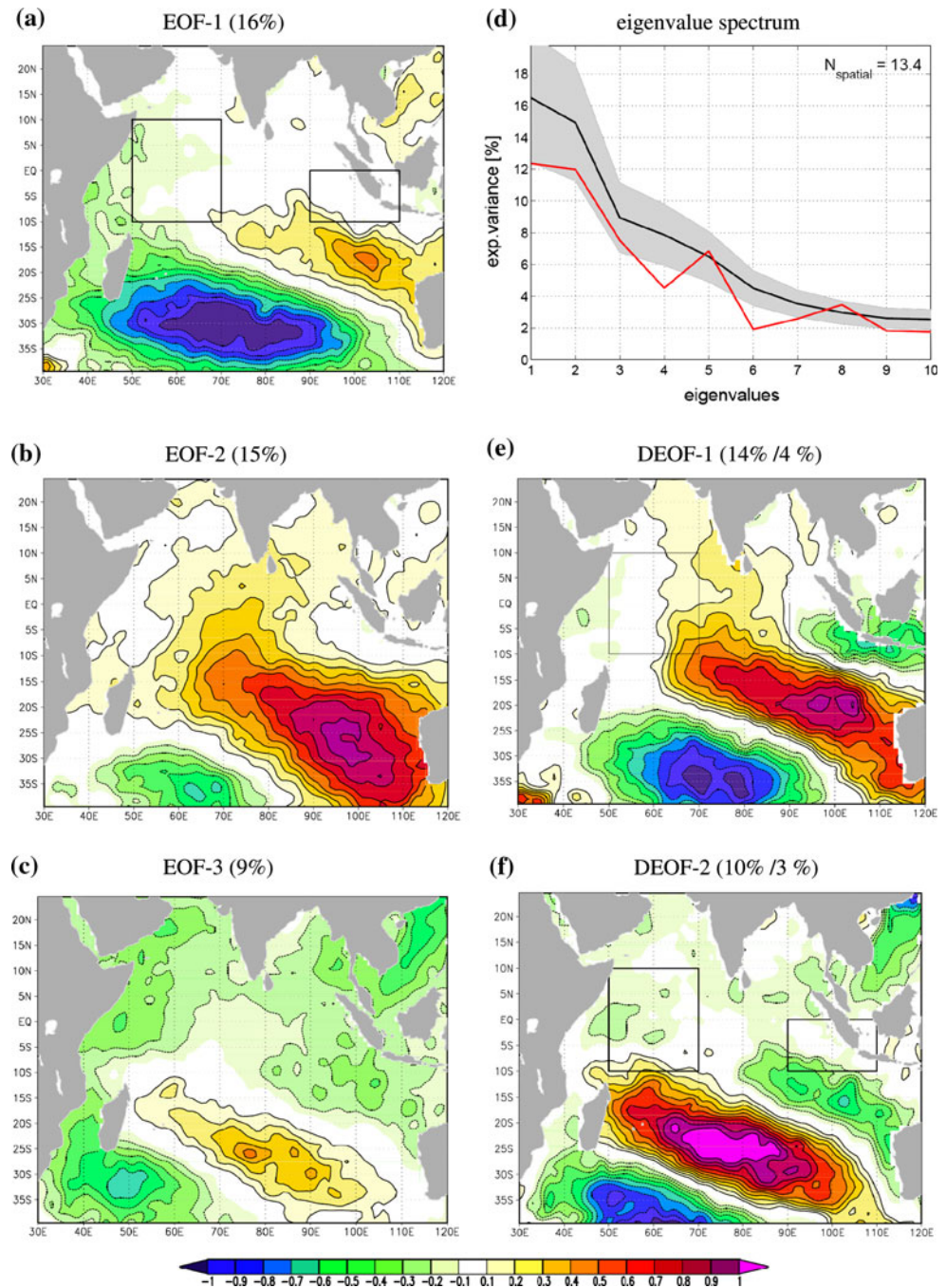


there in). It explains about 30% of the unfiltered and 40% of the linear detrended data. The variability lags the ENSO evolution behind and has seasonally evolving spatial structure. In the past the ENSO variability in the Indian Ocean was considered a passive response to the tropical Pacific (e.g. Latif and Barnett 1995; Venzke et al. 2000). However, recent studies find that the Indian and Pacific are a strongly coupled system, with

coupling in both directions (e.g. Wu and Kirtman 2004; Kug and Kang 2006; Dommenget et al. 2006; Wu and Kirtman 2004; Jansen et al. 2009). Thus it seems more reasonable to describe the ENSO-related part of the tropical Indian Ocean as part of the ENSO variability, rather than a passive response to ENSO.

- The second most dominant mode of variability is the warming trend of the tropical Indian Ocean. It explains

Fig. 12 As in Fig. 4, but for the linear detrended SST with the ENSO variability removed ($SST_{deENSOed}$) and a larger domain, reaching further south

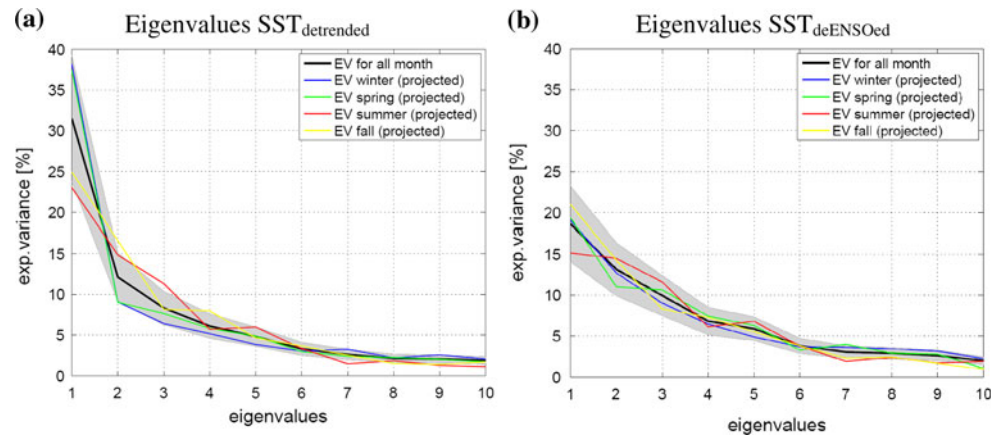


for about 24% of the variability, with its strongest amplitudes on the central equatorial Indian Ocean. It needs to be noted that this pattern is not orthogonal to the ENSO response pattern and both project onto the leading EOF-mode. The warming trend in the Indian Ocean is most likely a reflection of the anthropogenic climate change and will therefore most likely continue over the next decades.

- Further dominant modes of variability are two multipole patterns reaching from the extra-tropical south-

west to the equatorial Indonesia. They are related to the patterns discussed in the context of Australian droughts (e.g. Nicholls 1989; Ummenhofer et al. 2008). Since these patterns reach well into the southern extra-tropical regions, it seems very likely that these patterns are related to extra-tropical atmospheric variability, and are less related to internal tropical Indian Ocean variability, however, analyzing the causes of these patterns is beyond the scope of this article.

Fig. 13 **a** The eigenvalue spectrum of linear detrended SST as shown in Fig. 7, with the eigenvalues of the EOF-analysis restrict to each of the four seasons (colored lines) projected onto the all month eigenvalues (black line). **b** As in **a**, but for the linear detrended ENSO removed SST variability ($SST_{deENSOed}$), as shown in Fig. 9



- The residual (detrended, deENSOed and not considering the southern modes) SST variability has no dominant pattern of variability and may best be described by an isotropic diffusion process, which means that regional patterns of variability are dominating, which are of smaller than basin wide scale and are not related to coherent dipole or multi pole structures.
- The analysis presented here finds no evidence of the IOD mode or the leading role of the DMI other than that caused by the ENSO variability. None of the modes of variability found by the objective analysis presented here projects well onto the DMI. This also holds for the individual seasons. Although, the DMI projects on some EOF-modes (especially in the fall season), this is either due to the ENSO variability or it is a presentation of spatial red noise (isotropic diffusion), which has a domain wide dipole mode as one of the leading modes. As a reflection of spatial red noise the DMI cannot be interpreted as a coherent teleconnection between the two index regions. Rather it should be interpreted as variability in east–west direction with a specific length scale (see Dommenget 2007 for details). In summary it seems from this analysis, that the DMI is not a good index to describe tropical Indian Ocean SST variability.

Acknowledgments I like to thank Abdel Hannachi, and Noel Keenlyside for discussions and comments. This work was supported by the Deutsche Forschungsgemeinschaft (DFG) through the project DOI1038/2-1.

References

- Annamalai H, Liu P, Xie SP (2005) Southwest Indian Ocean SST variability: Its local effect and remote influence on Asian monsoons. *J Clim* 18:4150–4167
- Bader J, Latif M (2003) The impact of decadal-scale Indian Ocean sea surface temperature anomalies on Sahelian rainfall and the North Atlantic Oscillation. *Geophys Res Lett* 30:2169
- Baquero-Bernal A, Latif M, Legutke S (2002) On dipolelike variability of sea surface temperature in the tropical Indian Ocean. *J Clim* 15:1358–1368
- Barnett TP, Pierce DW, AchutaRao KM, Gleckler PJ, Santer BD, Gregory JM, Washington WM (2005) Penetration of human-induced warming into the world's oceans. *Science* 309:284–287
- Behera SK, Rao SA, Saji HN, Yamagata T (2003) Comments on “A cautionary note on the interpretation of EOFs”. *J Clim* 16:1087–1093
- Behera SK, Luo JJ, Masson S, Rao SA, Sakum H, Yamagata T (2006) A CGCM study on the interaction between IOD and ENSO. *J Clim* 19:1688–1705
- Bjerknes J (1969) Atmospheric teleconnections from the equatorial Pacific. *Mon Weather Rev* 97:163–172
- Bretherton CS, Widmann M, Dymnikov VP, Wallace JM, Blade I (1999) The effective number of spatial degrees of freedom of a time-varying field. *J Clim* 12:1990–2009
- Compo GP, Sardeshmukh PD (2010) Removing ENSO-related variations from the climate record. *J Clim* (in press)
- Deser C, Phillips AS, Hurrell JW (2004) Pacific interdecadal climate variability: linkages between the tropics and the North Pacific during boreal winter since 1900. *J Clim* 17:3109–3124
- Dommenget D (2007) Evaluating EOF modes against a stochastic null hypothesis. *Clim Dyn* 28:517–531
- Dommenget D, Latif M (2002) A cautionary note on the interpretation of EOFs. *J Clim* 15:216–225
- Dommenget D, Latif M (2003) Comments on “A cautionary note on the interpretation of EOFs”—reply. *J Clim* 16:1094–1097
- Dommenget D, Semenov V, Latif M (2006) Impacts of the tropical Indian and Atlantic Oceans on ENSO. *Geophys Res Lett* 33
- Hannachi A, Dommenget D (2009) Is the Indian Ocean SST variability a homogeneous diffusion process? *Clim Dyn* 33:535
- Hannachi A, Jolliffe IT, Stephenson DB (2007) Empirical orthogonal functions and related techniques in atmospheric science: a review. *Int J Climatol* 27:1119–1152
- Hasselmann K (1976) Stochastic climate models. Part 1: theory. *Tellus* 28:473–485
- Jansen MF, Dommenget D, Keenlyside N (2009) Tropical atmosphere-ocean interactions in a conceptual framework. *J Clim* 22:550–567
- Jolliffe IT (2002) Principal component analysis. Springer series in statistics, 2nd edn. Springer, New York
- Kalnay E, Kanamitsu M, Kistler R, Collins W, Deaven D, Gandin L, Iredell M, Saha S, White G, Woollen J, Zhu Y, Chelliah M, Ebisuzaki W, Higgins W, Janowiak J, Mo KC, Ropelewski C, Wang J, Leetmaa A, Reynolds R, Jenne R, Joseph D (1996) The NCEP/NCAR 40-year reanalysis project. *Bull Am Meteorol Soc* 77:437–471

- Kug JS, Kang IS (2006) Interactive feedback between ENSO and the Indian Ocean. *J Clim* 19:1784–1801
- Kug JS, Kang IS, Lee JY, Jhun JG (2004) A statistical approach to Indian Ocean sea surface temperature prediction using a dynamical ENSO prediction. *Geophys Res Lett* 31
- Latif M, Barnett TP (1995) Interactions of the tropical Oceans. *J Clim* 8:952–964
- Latif M, Dommenges D, Dima M, Grotzner A (1999) The role of Indian Ocean sea surface temperature in forcing east African rainfall anomalies during December–January 1997/98. *J Clim* 12:3497–3504
- Li T, Wang B, Chang CP, Zhang YS (2003) A theory for the Indian Ocean dipole-zonal mode. *J Atmos Sci* 60:2119–2135
- Mantua NJ, Hare SR, Zhang Y, Wallace JM, Francis RC (1997) A Pacific interdecadal climate oscillation with impacts on salmon production. *Bull Am Meteorol Soc* 78:1069–1079
- Marshall J, Kushner Y, Battisti D, Chang P, Czaja A, Dickson R, Hurrell J, McCartney M, Saravanan R, Visbeck M (2001) North Atlantic climate variability: phenomena, impacts and mechanisms. *Int J Climatol* 21:1863–1898
- Moller J, Dommenges D, Semenov VA (2008) The annual peak in the SST anomaly spectrum. *J Clim* 21:2810–2823
- Monahan AH, Fyfe JC, Ambaum MHP, Stephenson DB, North GR (2009) Empirical orthogonal functions: the medium is the message. *J Clim* 22:6501–6514
- Nicholls N (1989) Sea surface temperature and Australian winter rainfall. *J Clim* 2:965–973
- North GR, Bell TL, Cahalan RF, Moeng FJ (1982) Sampling errors in the estimation of empirical orthogonal functions. *Mon Weather Rev* 110:699–706
- Penland C, Matrosova L (2006) Studies of El Nino and interdecadal variability in tropical sea surface temperatures using a nonnormal filter. *J Clim* 19:5796–5815
- Rayner NA, Parker DE, Horton EB, Folland CK, Alexander LV, Rowell DP, Kent EC, Kaplan A (2003) Global analyses of sea surface temperature, sea ice, and night marine air temperature since the late nineteenth century. *J Geophys Res Atmos* 108
- Richman MB (1986) Rotation of principal components. *J Climatol* 6:293–335
- Saji NH, Goswami BN, Vinayachandran PN, Yamagata T (1999) A dipole mode in the tropical Indian Ocean. *Nature* 401:360–363
- Schott FA, Xie SP, McCreary JP (2009) Indian Ocean circulation and climate variability. *Rev Geophys* 47
- Shinoda T, Alexander MA, Hendon HH (2004) Remote response of the Indian Ocean to interannual SST variations in the tropical Pacific. *J Clim* 17:362–372
- Ummenhofer CC, Sen Gupta A, Pook MJ, England MH (2008) Anomalous rainfall over southwest Western Australia forced by Indian Ocean sea surface temperatures. *J Clim* 21:5113–5134
- Venzke S, Latif M, Villwock A (2000) The coupled GCM ECHO-2. Part II: Indian Ocean response to ENSO. *J Clim* 13:1371–1383
- Weare BC (1979) Statistical study of the relationships between Ocean surface temperatures and the Indian Monsoon. *J Atmos Sci* 36:2279–2291
- Webster PJ, Moore AM, Loschnigg JP, Leben RR (1999) Coupled ocean-atmosphere dynamics in the Indian Ocean during 1997–98. *Nature* 401:356–360
- Wu RG, Kirtman BP (2004) Understanding the impacts of the Indian Ocean on ENSO variability in a coupled GCM. *J Clim* 17:4019–4031
- Zebiak SE (1993) Air-sea interaction in the equatorial Atlantic region. *J Clim* 6:1567–1568